



Research Article

Adsorption performance of Pb(II) ions on green synthesized GO and rGO: Isotherm and thermodynamic studies

İkbal Gözde KAPTANOĞLU¹, Sabriye YUSAN²

¹Department of Materials Science and Engineering, Ege University, Graduate School of Natural and Applied Science, İzmir, Türkiye

²Ege University, Institute of Nuclear Sciences, İzmir, Türkiye

ARTICLE INFO

Article history

Received: 10 May 2022

Revised: 26 July 2022

Accepted: 21 August 2022

Key words:

Adsorption; Graphene oxide; Reduced Graphene Oxide; Pb(II) ion removal

ABSTRACT

Graphene oxide (GO) and reduced graphene oxide (rGO) are efficient and low-cost adsorbent carbon-based materials for removing Pb(II) ions from wastewater. In this article, the adsorption performance of environmentally friendly graphene oxide and reduced graphene oxide, which shows high adsorption capacity for Pb(II) ions, has been compared for the first time to our knowledge. Besides, the various characterization techniques are used such as X-ray diffraction, Fourier transform infrared spectroscopy, Raman spectroscopy and scanning electron microscopy with energy dispersive X-ray spectroscopy and described in detail as well. In addition, adsorption isotherms and thermodynamic studies are discussed to comprehend the adsorption process as well. From the adsorption isotherms, the maximum adsorption capacities of Pb(II) ions on GO and rGO calculated from the Langmuir (117.6 mg/g) and Dubinin–Radushkevich isotherms (138.5 mg/g), respectively, higher than reported studies in the literature. By thermodynamic investigation, it was found that the adsorption of Pb(II) ions on GO and rGO was spontaneous and exothermic. This study will be established as a basis for future studies and will be especially valuable in understanding the potential of graphene-based materials, which are rising stars that can be considered as promising and effective adsorbents in the removal of heavy metal ions from large volumes of aqueous solutions.

Cite this article as: Kaptanoğlu İG, Yusan S. Adsorption performance of Pb(II) ions on green synthesized GO and rGO: Isotherm and thermodynamic studies. Environ Res Tec 2022;5:3:257–271.

INTRODUCTION

Water is an indispensable part of the life cycle so that must need to be protected and conserved. Lead (Pb) ion is one of the most toxic heavy metals that pollutes water through the manufacture of paints, mining, fuels, storage batteries etc. [1].

Pb(II) ions, which threatens human health such as neurological disorders, kidney damage, anemia, and can even lead to death, is also very harmful for the environment and ecosystem [2, 3]. According to the United States Environmental Protection Agency (EPA), the allowable concentrations of lead in drinking water has been reported as 15 ppb [4].

*Corresponding author.

*E-mail address: gozdekaptanoglu@gmail.com



Graphene is an extraordinary material. It has a two-dimensional layer of carbon atoms arranged in a hexagonal crystal structure. Graphene and graphene-based materials have managed to attract the attention of researchers thanks to its magnificent properties such as high surface area, electron and thermal mobility, and mechanical strength [4]. Graphene oxide (GO) and reduced graphene oxide (rGO) and graphene-based composites, have recently attracted utmost attention in adsorption studies of in the removal of dye [5], heavy metal and radionuclide pollutants [6–8]. GO can be synthesized using various approaches such as Brodie [9], Staudenmaier, Hummers [10] by exfoliating the graphite via high oxidizing reagents. These procedures produce the toxic gases such as NO_2 , N_2O_4 and also being explosive. In addition to these methods, in 2010 Tour's et al. [11] reported an improve method of GO, in which the amount of KMnO_4 was doubled, included H_3PO_4 as well as H_2SO_4 . The biggest advantage of the Tour method is that it does not use NaNO_3 , which causes to the formation of toxic substances. GO has various oxygen-containing functional groups such as epoxy, hydroxyl and carboxyl in its basal plane and at its edges. These oxygen-containing groups combine metal ions and organic pollutants by coordination, electrostatic interaction, hydrogen bonding and this allows their use in pollution control [7].

It has been reported that most of the previous studies on the adsorption of heavy metals, GO synthesized by Hummer's method which produced toxic gases during the synthesis, and rGO synthesized with toxic reducing agent such as hydrazine and its derivatives [12, 13]. Although hydrazine is considered a good chemical reagent for rGO, in recent studies vitamin C (ascorbic acid) is considered to be an environmentally friendly and inexpensive reducing agent that can be used instead of hydrazine [14]. Also, the reduction performed by ascorbic acid is highly efficient and provides an advantage for large-scale production. Another advantage of using ascorbic acid is that the risk of incorporating heteroatoms into the structure is minimized, since it consists only of carbon, hydrogen and oxygen [14–16].

Researchers have reported extensive studies for the removal of Pb(II) ions from aquatic environments and various methods such as ion exchange, membrane filtration, electrodeposition, and coagulation have been studied [17, 18]. Adsorption is one of the most preferred methods among them thanks to its simple operation, low cost and applicable in large scale [19, 20]. Various type of adsorbents has been used to remove Pb(II) ions from aquatic environments such as zeolites [21], activated carbon [22], carbon aerogel [23], manganese oxide-coated carbon nanotubes [24], chitosan/magnetite composite beads [25], olive cake [26] etc.

Nowadays, cheap, effective and at the same time environmentally friendly adsorbent materials are needed to remove pollutants from aqueous solutions. Here, for the first time

our knowledge, GO was obtained by Tour method which is environmentally friendly method, and rGO was synthesized with non-toxic natural reducing agent L-ascorbic acid, and used as adsorbent materials to remove Pb(II) ions from the aquatic environment and their adsorption behavior was investigated. With this study, it was possible to obtain a green and economical adsorbent for the removal of Pb(II) ions from water. Characterizations of the resulting products were done by XRD, SEM-EDS, FT-IR and Raman spectroscopy. Adsorption experiments were investigated in detail under variable operating conditions such as pH, contact time, initial Pb(II) concentration and temperature of Pb(II) solutions. The obtained results were studied by Langmuir, Freundlich, Temkin and Dubinin-Radushkevich isotherm models. In addition, thermodynamic studies (enthalpy, entropy and Gibbs free energy) were calculated by experimental data for the both materials.

MATERIALS AND METHODS

Materials

Synthetic graphite powder ($<20\ \mu\text{m}$) was purchased from Sigma Aldrich. All chemical reagents, 95–98% sulfuric acid (H_2SO_4), 85% phosphoric acid (H_3PO_4), potassium permanganate (KMnO_4), 30% hydrogen peroxide (H_2O_2), 37% hydrochloric acid (HCl), Nitric acid (HNO_3), ammonia solution, L-ascorbic acid (L-AA), lead(II) nitrate ($\text{Pb}(\text{NO}_3)_2$), sodium hydroxide (NaOH), absolute ethanol, were analytical grade and purchased from Merck.

Preparation of Adsorbents

The GO was synthesized by chemical oxidation of graphite powder using Tour' method [11]. Briefly, 9:1 mixture of concentrated H_2SO_4 and H_3PO_4 (360:40 mL) were prepared and stirred for 15 minutes before adding graphite powder (3.0 g) with ice bath. After that, KMnO_4 (18.0 g) were gradually added into the mixture under the continuous stirring. Then the mixture was heated at $50\ ^\circ\text{C}$ and stirred for 12 h. After the reaction was cooled to room temperature and the mixture was poured onto ice (400 mL). Then, 30% H_2O_2 (3 mL) was added until the color of the reaction mixture turned to bright yellow. The brilliant yellow mixture was then repeatedly centrifuged at 4000 rpm and washed with HCl, deionized water, and ethanol. The final product of GO was dried an oven at $70\ ^\circ\text{C}$.

The as-dried GO sheet (0.45 g) was added into 500 mL deionized water and ultrasonicated for 1.0 h to homogenize the dispersion. As a reducing agent, L-ascorbic acid (4.5 g) was added to this solution and stirred with a magnetic stirrer for 1.0 h at room temperature. Afterward, pH of the suspension was adjusted to 9.5 using ammonia solution (25% w/w) to provide colloidal stability of GO sheet through electrostatic repulsion in alkaline conditions [27]. Then the mixture was heated at $70\ ^\circ\text{C}$ under magnetic stirring

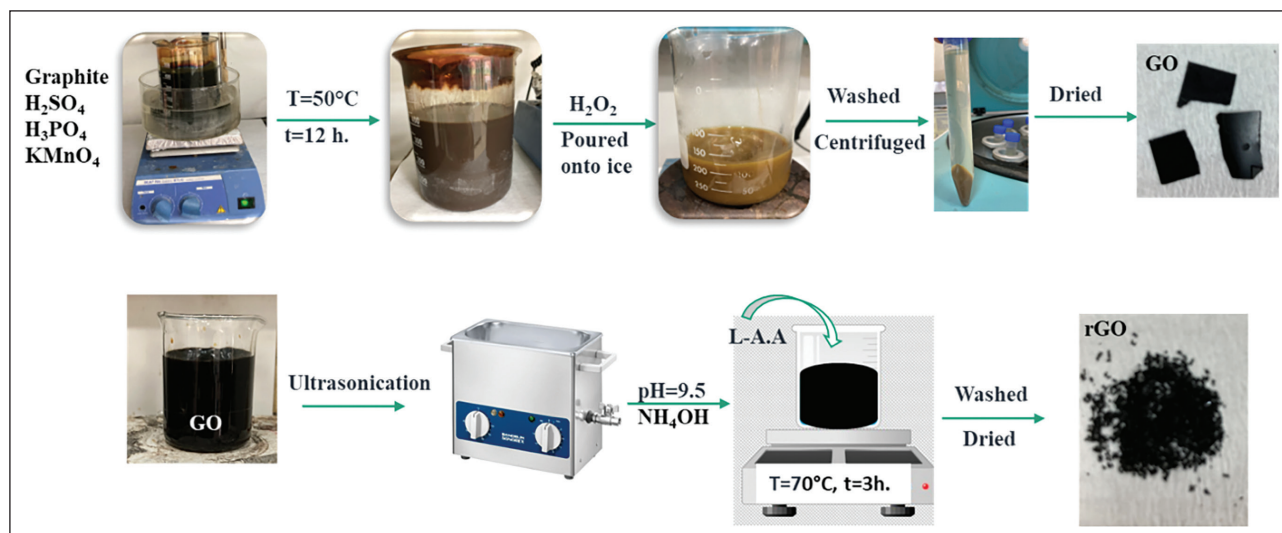


Figure 1. Photographs and schematic diagram for the preparation of GO and rGO.

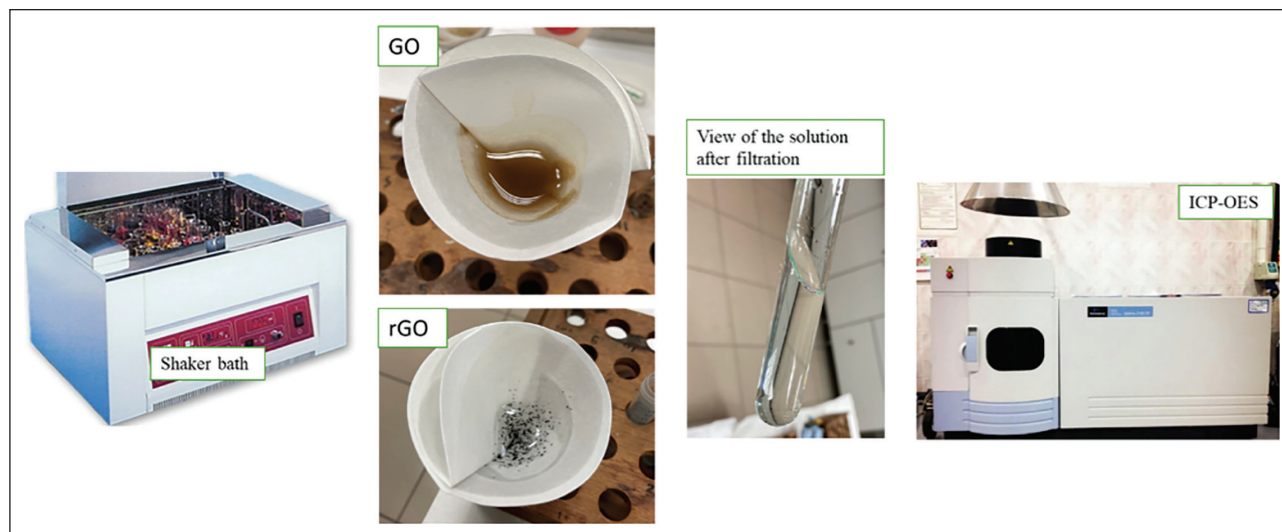


Figure 2. Photographs and schematic diagram of a batch adsorption process.

and kept for 3 h to obtain rGO. The reduced product was repeatedly centrifuged at 4000 rpm for 30 min to remove the supernatant and washed by deionized water to remove residual L-AA. Finally, rGO was dried an oven at 70 °C. Preparation steps of GO and rGO are shown in Figure 1.

Batch Experiment

In this study, initial pH of the solution, initial concentration, contact time and temperature were investigated for the removal of Pb(II) ions by using GO and rGO as adsorbents during the batch adsorption experiment. Generally, the pH of 10 mL solution of known lead concentration was adjusted by adding dropwise with negligible amount of 0.1M NaOH and/or HCl. Then, adsorbent (0.01 g) was added into the solution and transferred into the electronic shaker bath. After achieving the adsorption equilibrium for

a certain period of time, the solid parts were removed from the liquid part immediately by the aid of a filter.

Figure 2 shows the scheme of batch experimental stage. After adding GO to Pb(II) solutions, GO is dispersed in the solution due to the hydrophilic nature of GO although rGO does not disperse because it is hydrophobic. After the filtration, a clear and transparent solution was observed for both and the remaining Pb(II) ion concentration was measured by ICP-OES.

The adsorption capacities and removal percentage rate were calculated as follows:

$$q_e = \frac{C_i - C_e}{m} \times V \tag{1}$$

$$\text{removal percentage rate(\%)} = \frac{C_i - C_e}{C_i} \times 100 \tag{2}$$

where C_i and C_e in mg/L represent the initial and equilibrium Pb(II) concentration, respectively; V (L) is the volume of the solution in the adsorption study; and m (g) is the mass of adsorbent used.

Analysis Methods

X-ray diffraction (XRD) analysis was carried out on an X-ray diffractometer (Malvern Panalytical Empyrean) with Cu $K\alpha$ radiation ($\lambda=1.5406$) at 45 kV and 40 mA with a step size of 0.01 and recorded in the 2θ range of 5–60°. The chemical characterization of the samples was analyzed by Fourier transform infrared spectroscopy-attenuated total reflectance (FTIR-ATR) spectrophotometer (Perkin Elmer) and Raman spectra (Renishaw Raman spectrometer) with a 532 nm laser wavelength. It was recorded at the wavenumber region of 4000–450 cm^{-1} and the Raman Shift region of 3000–1000 cm^{-1} corresponding to FTIR and Raman spectrums. The morphological characterization of the samples was captured from a scanning electron microscopy (SEM) (Carl Zeiss 300VP) and elemental compositions were determined by energy-dispersive X-ray spectroscopy (EDS). The operational details of characterization methods can refer to the literature [28, 29]. All batch adsorption experiments were carried out in a thermostated electronic shaker bath (GFL 1083). The pH values of aqueous solutions were measured by a Hanna Instrument, model 8521, pH meter. The measurements of residual Pb(II) concentration were performed using inductively coupled plasma optical emission spectrometry (ICP-OES) (Perkin Elmer Optima DV 2000).

RESULTS AND DISCUSSION

Characterization of Synthesized Adsorbents

In this study, Tour method was used to synthesize graphene oxide by using graphite as a starting material. After the oxidation process, GO was reduced by using L-ascorbic acid as a non-toxic reducing agent.

XRD analysis was used to understand phase formation and verify the interlayer spacing of graphite, GO and rGO samples.

The interlayer spacing of samples can be calculated according to the Bragg law:

$$n\lambda = 2d\sin\theta \quad (3)$$

where n is an integer, λ is wavelength of X-ray for the copper target, θ is angle between the incident and reflected rays and d is the interlayer distance or d-spacing of Miller indices.

The crystallite size of the sample can be calculated using the Debye-Scherrer equation from the following equation:

$$D = \frac{K\lambda}{\beta\cos\theta} \quad (4)$$

where D is the crystallite size of the sample, K is the Scherrer constant (0.94), λ is the wavelength of Cu- $K\alpha$ (1.54 Å), β is the half-width (rad) of the X-ray diffraction peak (FWHM), and θ is the Bragg's diffraction angle.

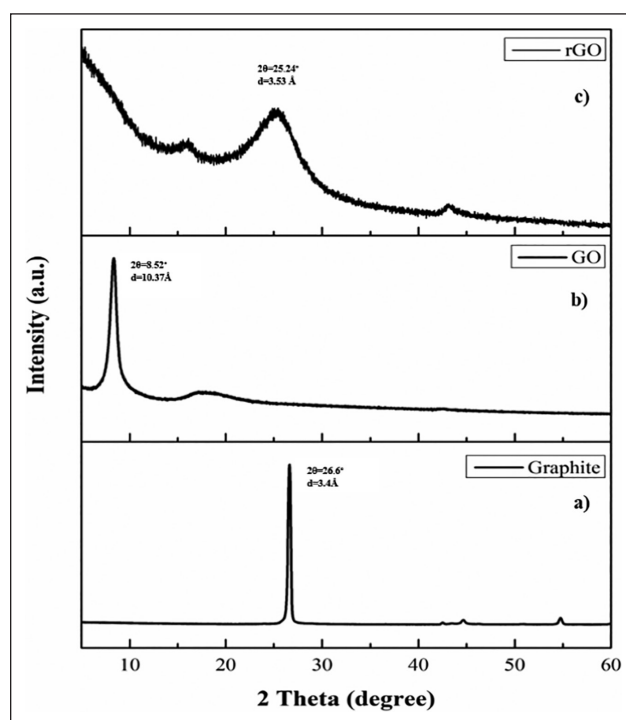


Figure 3. XRD patterns of graphite (a), graphene oxide (b) and reduced graphene oxide (c).

Figure 3a shows the XRD spectra of graphite as a starting material. The interlayer spacing of graphite was calculated from the characteristic peak where is a very sharp peak at $2\theta=26.6^\circ$ along with the orientation at (002) plane comes out to be 3.4 Å which is similar in literature [30]. The characteristic graphite peak is disappeared after oxidation process in the synthesized GO as shown in Figure 3b. The characteristic peak of GO at $2\theta=8.52^\circ$ from the diffraction of the (001) plane comes out to be 10.37 Å which is in good agreement with the literature [31]. By comparing graphite and GO, the reason of shifting 2θ values from the 26.6° to 8.52° is that the d-spacing between carbon layers increased with the addition of functional groups in oxidation process and graphite is fully oxidized to GO [31]. It can be seen that the characteristic peak position $2\theta=25.24^\circ$ from the diffraction of the (002) was the confirmation of reduction of graphene oxide in Figure 3c. The d-spacing of rGO was calculated using Bragg's law to be 3.53 Å. After the reduction process, the interlayer distance of rGO was lower than GO that infers oxygen containing functional groups were removed efficiently [32]. This result clearly indicate that L-ascorbic acid is an effective reducing agent for GO reduction.

Results from the XRD patterns and Debye-Scherrer equation, the average number of layers was calculated equation 5. In our case, synthesized GO has ~9 scattering layers while rGO has ~5.

$$n = D/d \quad (5)$$

Table 1. Results of XRD analysis for graphite, graphene oxide and reduced graphene oxide samples

Sample name	2 Theta (°)	Interlayer distance (Å)	FWHM (°)	Crystallite size (nm)	Number of layers
Graphite	26.6	3.4	0.34	25.02	74.7
GO	8.52	10.37	0.86	9.68	9.33
rGO	25.24	3.53	5.13	1.65	4.69

where n is the number of layers, D is the crystallite size of the sample calculated using the Debye-Scherrer equation and d is the interlayer distance between the planes.

XRD analysis results which are including 2θ , interlayer spacing, FWHM, crystallite size and number of layers of graphite, GO and rGO are given in Table 1 Results of XRD analysis for graphite, graphene oxide and reduced graphene oxide samples.

FT-IR spectrum give the information of functional groups in graphite, GO and rGO. In Figure 4a, the FT-IR spectrum of graphite is given and clearly seen that do not show any peaks means no oxygen bonds are observed [33]. After the oxidation process, it is seen that FT-IR spectrum of GO in Figure 4b show that oxygen-containing functional groups are introduced in the structure. The FT-IR peaks of GO at 1040, 1219, 1383, 1622, 1729 and 3220 cm^{-1} , which are vibration of alkoxy C–O, epoxy C–O, attributed to the O–H deformation vibration of COOH group, C=C skeletal stretching, carboxylic acid –C=O, and hydroxyl –OH groups, respectively [34]. The FT-IR spectrum of GO show that the existence functional groups designate that graphite has been oxidized and the polar groups particularly hydroxyl groups, made the GO form hydrogen bonds with water molecules and provide hydrophilic nature. The reduction of the oxygen-containing groups in GO by L-AA was also proven by FT-IR spectroscopy as shown in Figure 4c.

After the reduction of graphene oxide, intensities of the peaks corresponding to the oxygen functionalities such as hydroxyl–OH peak at 3660 cm^{-1} were reduced significantly and some peaks were disappeared such as –COOH stretching vibration peak at 1741 cm^{-1} . These results indicates that the GO has been reduced by ascorbic acid. Similar results have been reported in the literature [35, 36].

In Figure 5, surface morphology and elemental composition of graphite, GO and rGO was examined by SEM and EDS spectrum, respectively. Graphite is shown in a platelet-like stacked sheets (Fig. 5a) while GO has wrinkle, layered and folded morphology (Fig. 5b). The reason for the formation of these morphology is due to the oxygen-containing functional groups formed during the GO formation and the consequent structural defects [37]. SEM images of rGO in Figure 5c show wrinkled, wavy and aggregated morphology. According to EDS results as shown in Figure

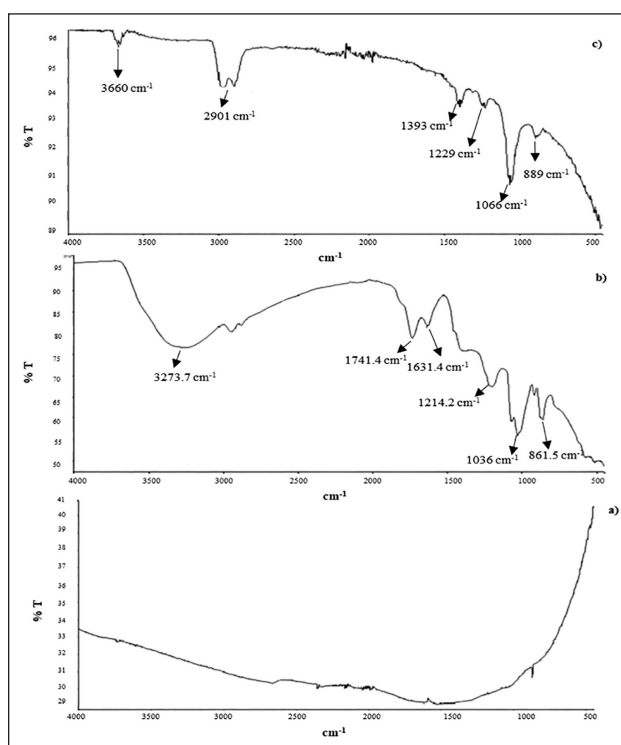


Figure 4. FT-IR spectrums of graphite (a), graphene oxide (b) and reduced graphene oxide (c).

5d, graphite contained almost only C (98.4%) by weight. After the oxidation process, GO (Fig. 5e) consisted of both C (44.8%) and O (51.4%) peaks with carbon/oxygen (C/O) ratio was calculated to be 0.87. In comparison, rGO (Fig. 5f) contained larger amounts of carbon (76.8%) relative to oxygen (23.2%). It is understood that with the reduction of GO to rGO with ascorbic acid, the functional groups deteriorate and the C percentage increases and the C/O ratio increases from 0.87 to 3.31. C/O ratios may differ according to synthesis and reduction methods [38].

Raman spectroscopy is a very useful technique to characterize carbon-based materials. The typical Raman spectrum of carbon materials composed of D, G and 2D bands. While D band is appeared in near 1350 cm^{-1} , G and 2D bands are appeared in near 1580 cm^{-1} and 2700 cm^{-1} , respectively. Those Raman bands give different information. Briefly, D band is related to defects vibrations of sp^3 carbon atoms of defects and disorder in the material, G band is related to vibration of sp^2 carbon atoms in a graphitic 2D hexagonal lattice and 2D band is related to number of graphene layers [39].

The Raman spectrum of graphite, prepared GO and rGO is shown in Figure 6. D band of graphite has a low-intensity compared to the G band which is related with nanocrystalline carbon in presented Figure 6a. Besides, graphite has a high intense of 2D band. The I_{2D}/I_G ratio=0.36 indicates the presence of multilayers of graphite as reported similar

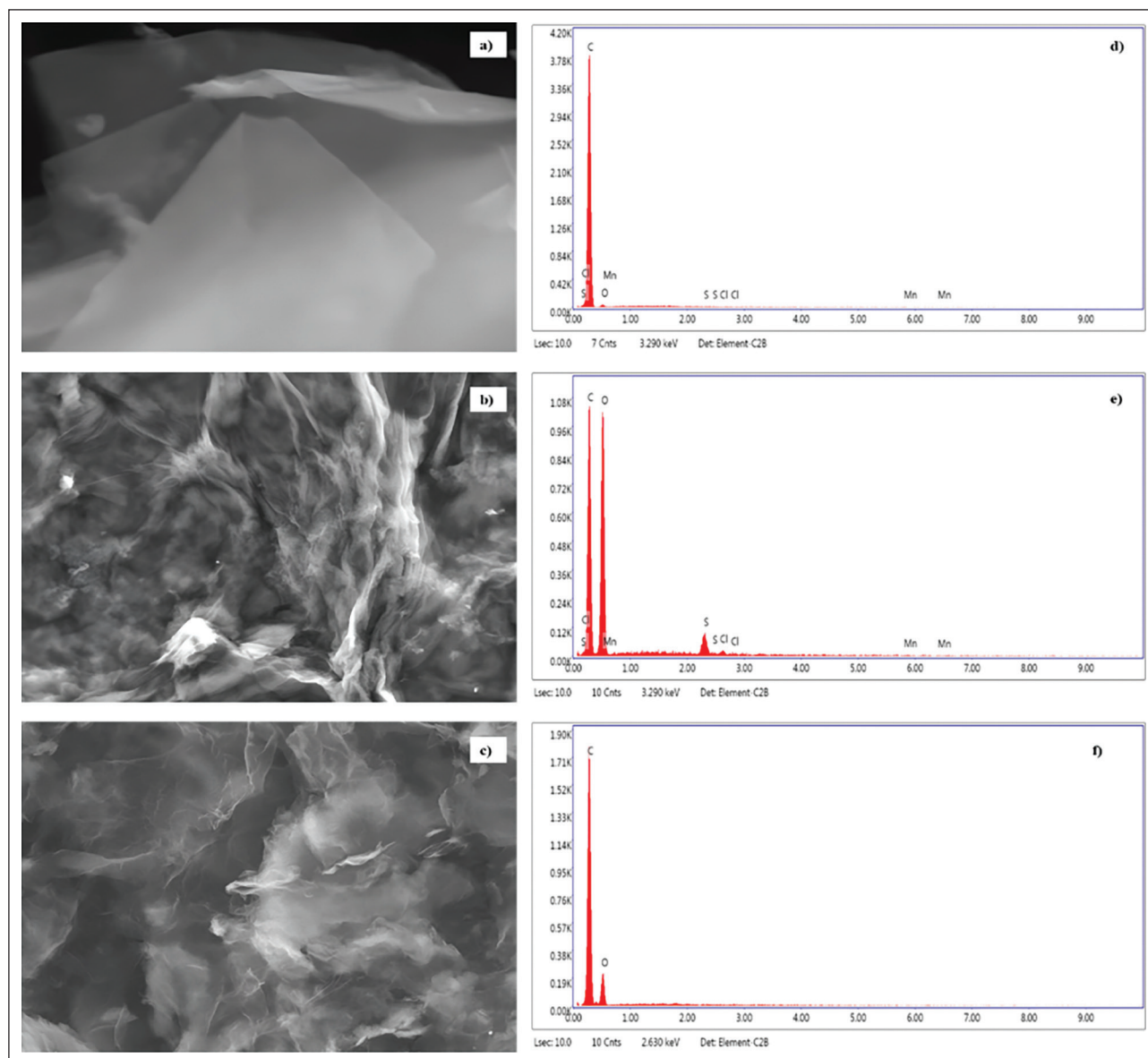


Figure 5. SEM images of graphite (a), graphene oxide (b) and reduced graphene oxide (c) and EDS spectrum of graphite (d), graphene oxide (e) and reduced graphene oxide (f).

[40]. By comparing graphite and GO, it is obviously seen that more intense D band observed in Figure 6b. A common way to describe the defect density in a material is the ratio of the intensities of the D-band to the G-band. A value of the $I_D/I_G=0.91$ indicates greater disorder of the basal planes of the GO due the functional groups present on the surface of each layer. This is an indication of the increment of disordered phase in the GO in consequence of the oxidation of graphite and related to the formation of sp^3 hybridized bonds. In addition, flat and low intensity of 2D band observed. These properties support the disorder of the material layers and show that GO is composed of multilayers according to $I_{2D}/I_G=0.04$. After the reduction process, it was found that the intensity ratio D band to G band ($I_D/I_G=1.11$)

increased significantly. This result indicates that most of the oxygenated groups vanished during the reduction process. Similar results have been reported in the literature [35].

Pb(II) Adsorption Evaluations on Synthesized Adsorbents

The influence of initial pH, concentration, contact time and temperature on the adsorption of Pb(II) ions was studied by adding 0.01 g of GO and rGO as adsorbents and 10.0 mL of sample solution into the tubes. The solutions prepared to be studied at different pH values, initial concentrations, different time intervals and temperatures were transferred to the tubes and shaken in a temperature-controlled shaker. Experiments were performed with other conditions held constant.

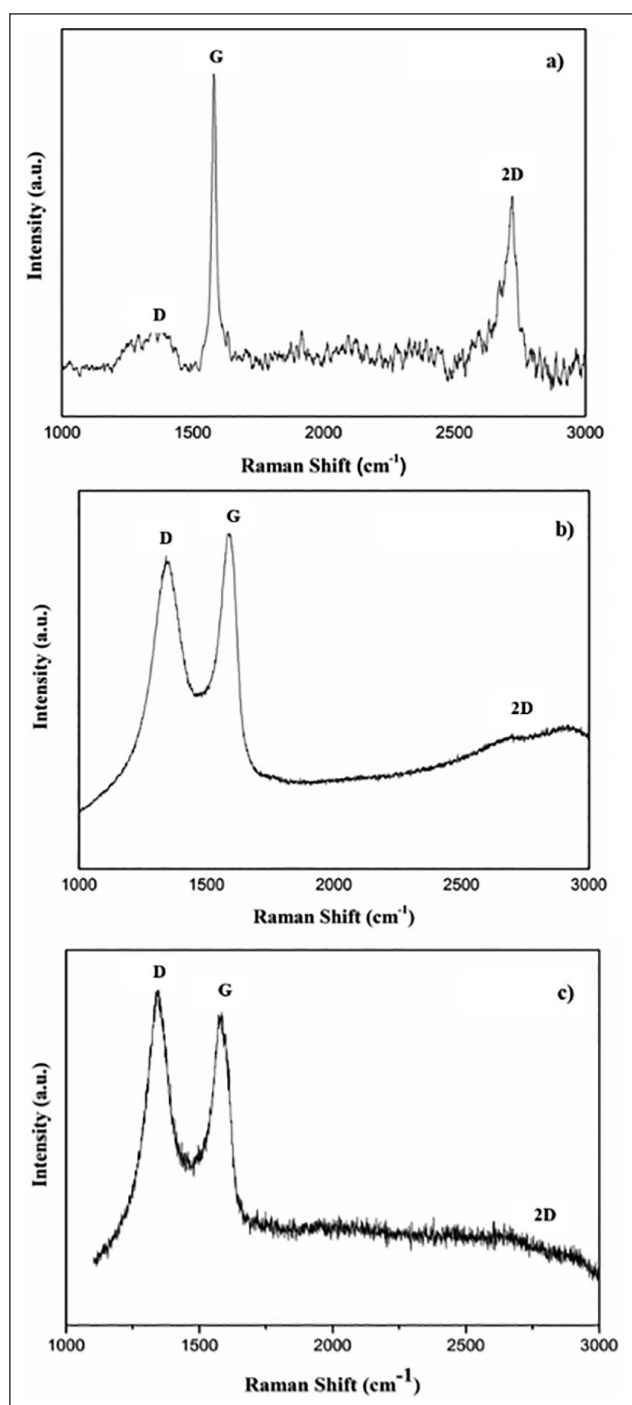


Figure 6. RAMAN spectra of graphite (a), graphene oxide (b) and reduced graphene oxide (c).

The role of solution pH is very important to remove the adsorbents from aqueous solutions. Because it affects the surface charge of the adsorbent and states of the functional groups of adsorbents as well as the adsorbate [41]. To study the influence of pH upon % removal rate of Pb(II) of synthesized materials, the experiments were conducted in the pH range of 3–6 at room temperature with 100 mg/L lead

and the equilibrium time was kept 30 minutes. Equilibrium solution pH of adsorbent was measured by a portable pH meter. In the Pb(II) adsorption process, alkaline pH should be avoided as precipitation occurs instead of adsorption, therefore above the pH 6.00 were not studied [42].

The results of the experiment are shown in Figure 7. Maximum removal rate was obtained 69% and the adsorption capacity (69.3 mg/g) was the highest at pH 4.0 for GO. On the other hand, Pb(II) removal rate for rGO was higher than GO. rGO has 89% removal rate with the adsorption capacity was calculated 88.94 mg/g at pH 4.0. Since the values obtained at pH 5.0 and 6.0 were very close to pH 4.0, the studies were continued with pH 4.0 for rGO. In the current study, pH value of 4.0 was chosen as optimum.

Figure 8 shows the effects of different initial concentration of Pb(II) on the adsorption of the GO and rGO surface. Throughout the study, the initial lead concentration was studied from 25 to 250 mg/L at room temperature and the equilibrium time was kept 30 minutes at pH 4.0. The removal rate of Pb(II) decreases and the adsorption capacity increases with an increase in initial Pb(II) concentration. It may be due to an increase in the number of Pb(II) ions for the fixed amount of adsorbent. The decrease in percentage removal can be clarified that all the adsorbents had a limited number of active sites, that would have become saturated above a certain concentration. The amount of Pb(II) adsorbed per unit mass of GO and rGO increases with increase in Pb(II) concentration, may be due to the complete utilization of adsorption surface and active sites available which is not possible in low concentration. For the rGO, the optimum values of Pb(II) removal and adsorption capacity are found to be 89% and 88.94 mg/g, respectively, with the initial Pb(II) concentration value of 100 mg/L. For the GO, the optimum values of Pb(II) removal and adsorption capacity are found to be 70.9% and 35.48 mg/g, respectively, with the initial Pb(II) concentration value of 50 mg/L.

Adsorption is highly a time dependent process. When the adsorbent and adsorbate are contacted for a sufficient time, the adsorption performance will increase as the interaction between the ions will ensure the completion of the adsorption process. For this reason, it is very important that the adsorbent and Pb(II) ion have sufficient contact time and reach equilibrium in order to complete the adsorption reaction [2, 42]. In order to study the effect of contact time on adsorption of Pb(II) on GO and rGO was investigated to determine the equilibrium contact time shown in Figure 9.

Removal efficiency was observed to increase as the contact time was increased from 5 to 240 minutes. The uptake of Pb(II) onto GO was rapid within the first 60 minutes due to the availability of binding sites and greater concentration gradient. However, no considerable increase was observed on the removal efficiency as the contact time was further

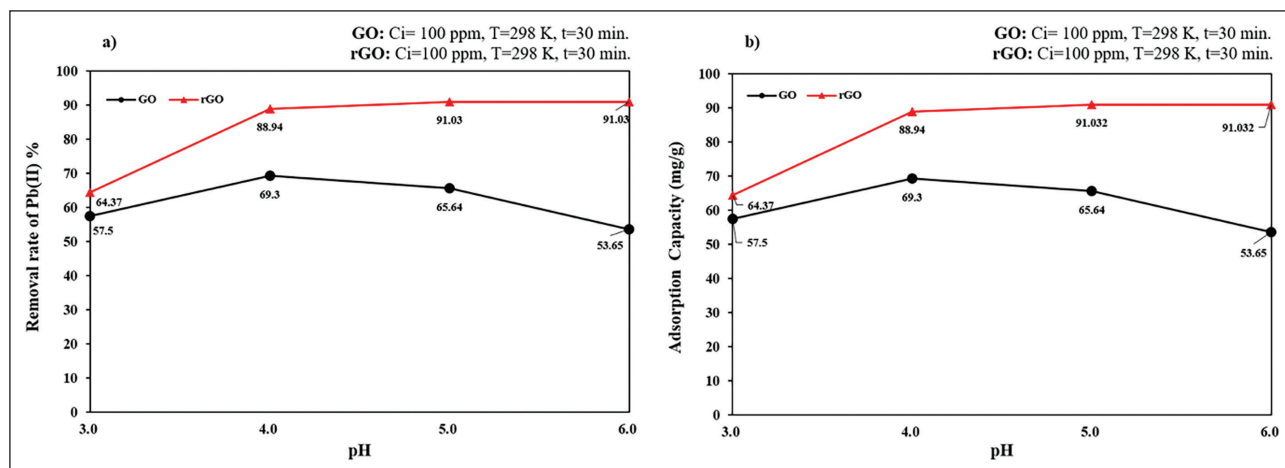


Figure 7. Effect of pH on removal rate (a) and adsorption capacity (b) onto the GO and rGO materials.

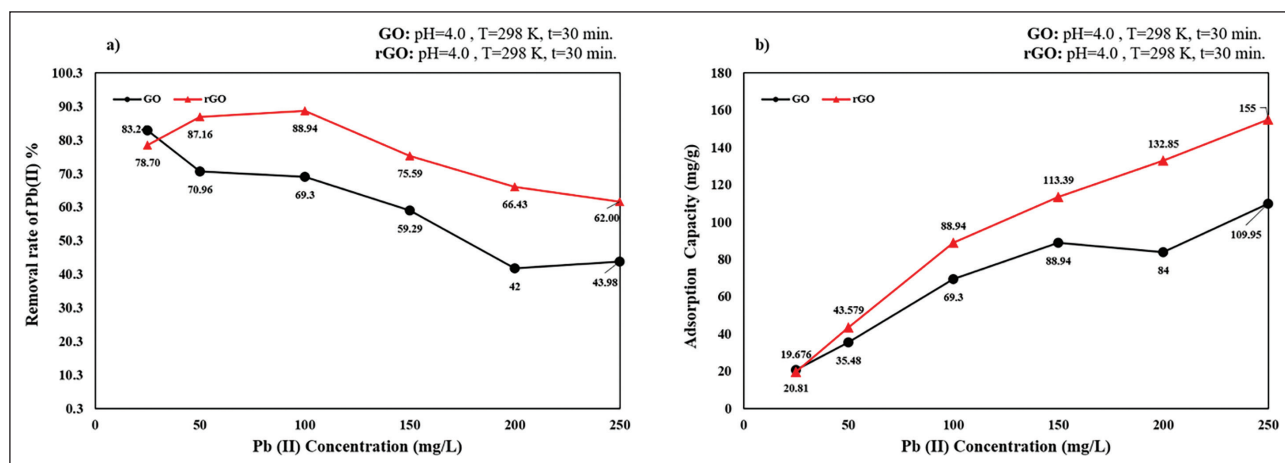


Figure 8. Effect of initial Pb(II) concentration on removal rate (a) and adsorption capacity (b) onto the GO and rGO materials.

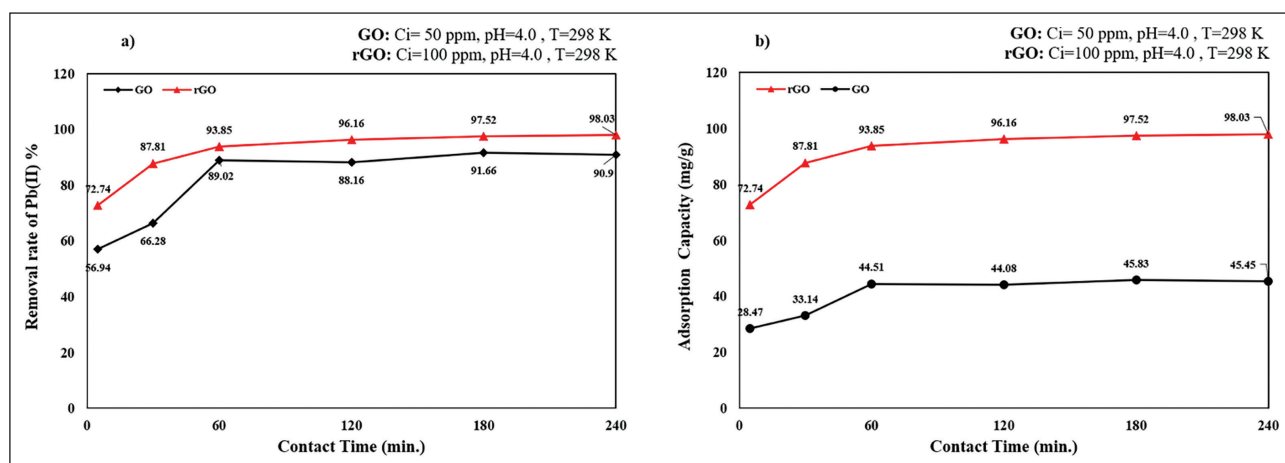


Figure 9. Effect of contact time on removal rate (a) and adsorption capacity (b) onto the GO and rGO materials.

increased from 60 to 240 minutes. Equilibrium was attained at 60 min. with maximum removal efficiency 89% with the adsorption capacity was calculated 69.3 mg/g for GO while

94% with the adsorption capacity was calculated 93.9 mg/g for rGO. In the present work, 60 min was selected as the contact time to ensure equilibrium.

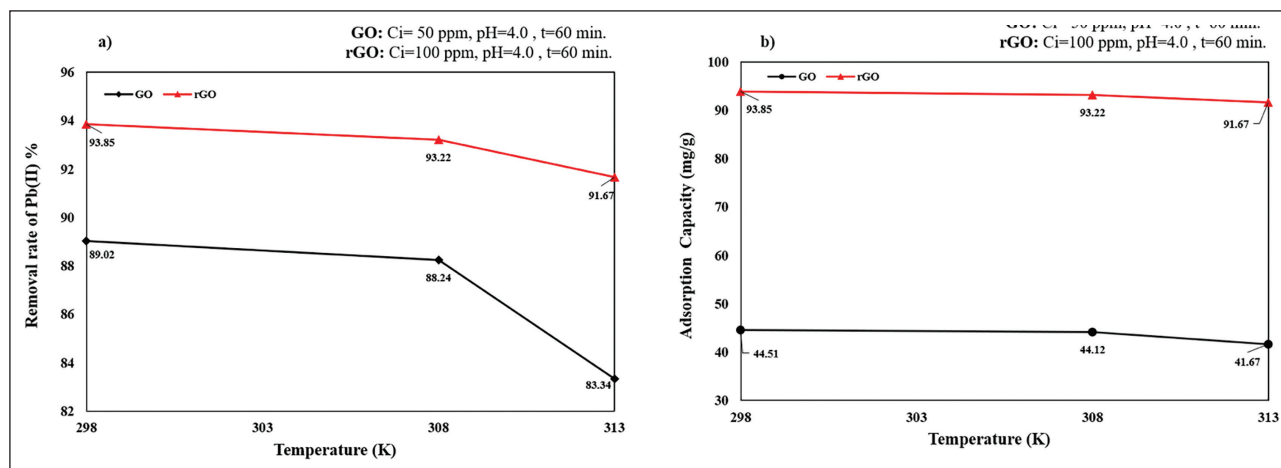


Figure 10. Effect of temperature on removal rate (a) and adsorption capacity (b) onto the GO and rGO materials.

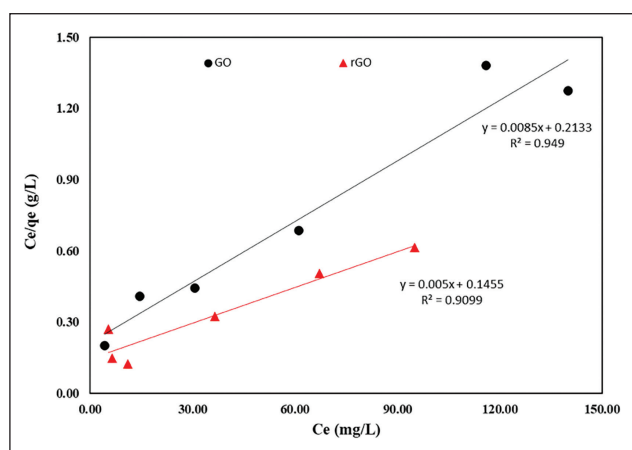


Figure 11. Langmuir plots for adsorption of Pb(II) by the GO and rGO materials.

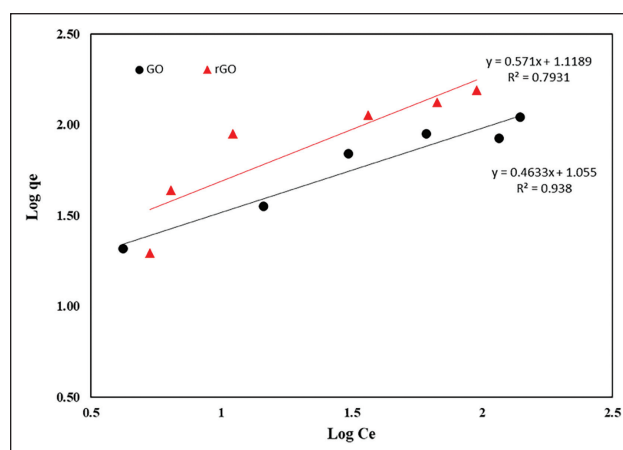


Figure 12. Freundlich plots for adsorption of Pb(II) by the GO and rGO materials.

To understand the effect of temperature, experiments at 298, 308 and 313 K were conducted and the results are shown in Figure 10. It has been seen that removal percentage of Pb(II) slightly decrease when the temperature increase. The adsorption process is more favorable at room temperature for both adsorbents.

Adsorption isotherms can be used to understand the interactions between an adsorbate and sites on the sorbent surface [43]. The Pb(II) solutions in the range of 25–250 mg/L was used to study the adsorption isotherms. Adsorption isotherms are represented by the Langmuir, Freundlich, Temkin and Dubinin-Radushkevich models with the results shown in Table 2.

The Langmuir isotherm (Fig. 11) is widely used model that describes adsorption on homogeneous surface by monolayer sorption without interaction between adsorbed molecules [26, 44].

The linear form of Langmuir equation can be expressed as follows:

$$\frac{C_e}{q_e} = \frac{1}{K_L q_m} + \frac{C_e}{q_m} \tag{6}$$

where C_e (mg/L) is the equilibrium concentration, K_L (L/mg) is the Langmuir constant and q_m (mg/g) is the maximum adsorption quantity.

The favorability of adsorption can be expressed by factor R_L in equation 7. The R_L values indicate that the adsorption process is favorable when $0 < R_L < 1$, unfavorable when $R_L > 1$ and irreversible when $R_L = 0$ [45].

$$R_L = \frac{1}{1 + K_L C_i} \tag{7}$$

The Freundlich isotherm is based on heterogeneous adsorption process calculated by the equation 8 when plotted as $\log q_e$ versus $\log C_e$ (Fig. 12).

$$\log q_e = \log K_f + \frac{1}{n} \log C_e \tag{8}$$

where K_f and $1/n$ are the Freundlich constants. The value of n ranging from 1 to 10 indicated that the adsorption process is favorable [46].

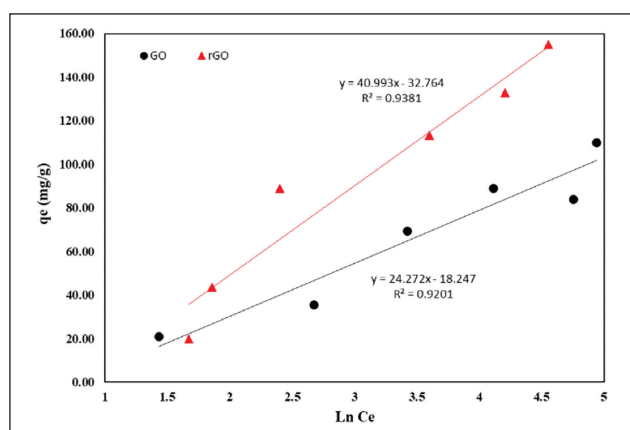


Figure 13. Temkin plots for adsorption of Pb(II) by the GO and rGO materials.

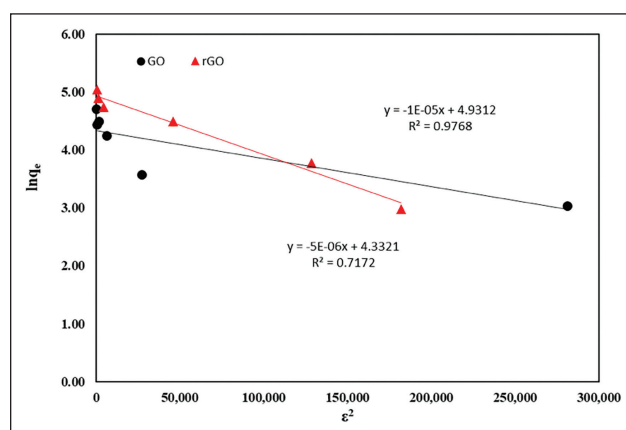


Figure 14. Dubinin-Radushkevich plots for adsorption of Pb(II) by the GO and rGO materials.

Table 2. Adsorption isotherm parameters of Pb(II) adsorption on GO and rGO

Isotherm models	Parameters	GO	rGO
Langmuir	q_m (mg/g)	117.647	200.000
	K_L (L/mg)	0.040	0.034
	R_L	0.334	0.225
	R^2	0.949	0.910
Freundlich	n	2.158	1.751
	K_f	11.350	13.149
	R^2	0.938	0.793
Temkin	b_T (J/mol)	24.272	40.993
	K_T (L/mg)	0.472	0.450
	R^2	0.920	0.938
Dubinin–Radushkevich	K_{DR} (mol/KJ) ²	0.00000500	0.00001014
	q_m (mg/g)	76.104	138.540
	E (kJ/mol)	316.228	222.014
	R^2	0.717	0.971

The Temkin isotherm (Fig. 13) is related to adsorbate and adsorbent interaction and based on this model, the temperature-dependent heat of adsorption of all molecules on the sorbent surface decreases linearly due to interactions with represent the following equation [43].

$$q_e = B \ln K_T + B \ln C_e \quad (9)$$

$$B = \frac{RT}{b_T} \quad (10)$$

where b_T is the Temkin constant related to the heat of adsorption [J/mol] and K_T represents the Temkin isotherm equilibrium binding constant [L/mg] corresponding to the maximum binding energy.

Dubinin–Radushkevich (D–R) (Fig. 14) is another model which is used to apparent free energy of adsorption, ad-

sorption mechanism based on potential theory which assumes the porous structure and heterogeneous surface of the sorbent [47]. The linear form of D-R isotherm equation is given at the following [46].

$$\ln q_e = \ln q_m - K_{DR} \epsilon^2 \quad (11)$$

$$\epsilon = RT \ln \left(1 + \frac{1}{C_e} \right) \quad (12)$$

$$E = \frac{1}{\sqrt{-2\beta}} \quad (13)$$

where q_m (mg/g) is the adsorption capacity, K_{DR} (mol K/J)² is a constant related to energy, ϵ is the Polanyi potential, R is a gas constant (8.314 J/mol K), T is the absolute temperature (K), E is the adsorption mean energy. Plotting $\ln q_e$ against ϵ^2 , the values K_{DR} and q_m can be calculated from the slope and intercept, respectively.

It can be seen from the Table 2 in accordance with the value of R^2 , GO is fitted well by Langmuir isotherm with a maximum monolayer adsorption capacity 117.6 mg/g, while Dubinin–Radushkevich model shows a good agreement for rGO with a maximum adsorption capacity 138.5 mg/g. From the data calculated in Table 2, the R_L value of both GO and rGO are between 0–1 indicating that Langmuir isotherm is favorable. In addition, it is observed that the values of the Freundlich isotherm constant “ n ” are greater than 1, that means Pb(II) is favorably adsorbed onto GO and rGO. The calculated E value is used to predict the reaction mechanism of the adsorption process. If the E value is less than 8 kJ/mol, it indicates a physical adsorption, while the E value is higher than 8 kJ/mol, the adsorption process is chemical in nature [48]. In our cases, E value is 222 kJ/mol that means adsorption process is chemical in nature for rGO.

In Figure 15, the adsorption capacities obtained from the experimental and isotherm models are plotted. As seen in Figure 15a, Langmuir model shows better fit for GO while D-R model can be considered more proper for rGO in Figure 15b.

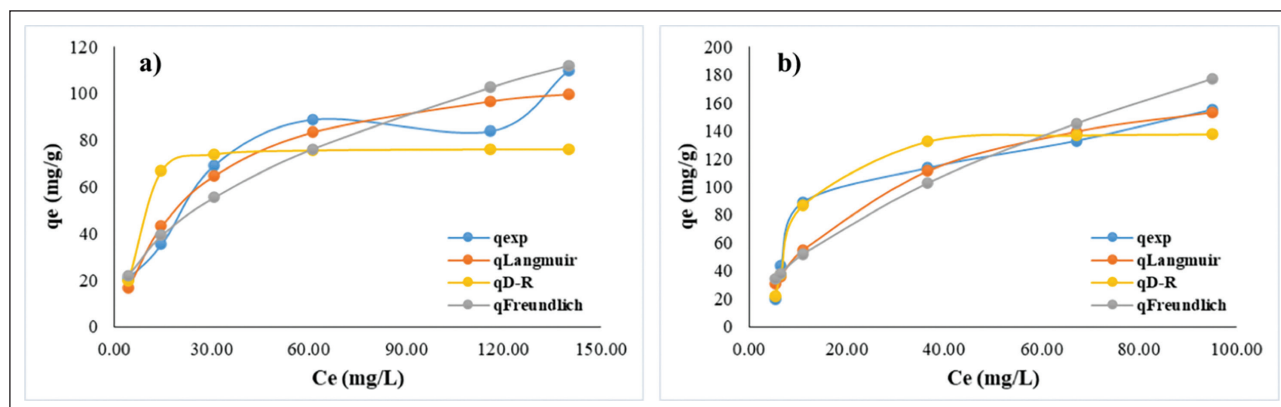


Figure 15. Comparison of adsorption capacities found from experimental and isotherm models for (a) GO and (b) rGO.

Table 3. Comparison of the maximum adsorption capacity of Pb(II) with various graphene-based adsorbents

Carbon-based adsorbent	Synthesis method	Isotherm model	Q _{max} (mg/g)	Reference
GO	Tour's	Langmuir	117.6	This work
rGO	Green Reduction by L-Ascorbic Acid	Dubinin–Radushkevich	138.5	This work
Graphene nanosheet	Vacuum-promoted low- temperature exfoliation	Langmuir	22.42	[49]
Graphene aerogel	Modified Hummer's	-	80.0	[50]
Polydopamine coated GO	Modified Hummer's	Langmuir	53.6	[51]
GO– Chitosan	Modified Hummer's	Freundlich	90.0	[52]
rGO-Mn3O4NC	Modified Hummer's chemical reduction followed by hydrothermal treatment	-	105.39	[53]
SiO ₂ /graphene	Hummer's	Langmuir	113.6	[54]

In this study shows higher Pb(II) capacities than other reported values for Pb(II) removal as mentioned in Table 3. These results suggests that graphene-based materials synthesized by environmentally friendly methods show great potential to remove Pb(II) ions in water pollution control applications.

The thermodynamic parameters that are ΔH^0 , ΔS^0 , and ΔG^0 for Pb(II) on GO and rGO were calculated from the temperature dependent adsorption isotherms. The related equations are shown from the following equations.

$$\Delta G^0 = -\ln K_L \quad (14)$$

$$\ln K_L = \frac{\Delta S^0}{R} - \frac{\Delta H^0}{RT} \quad (15)$$

where ΔH^0 is the standard enthalpy change, ΔS^0 is the standard entropy change and ΔG^0 is the standard free energy change R is the ideal gas constant (8.314 J/mol K), T is the absolute temperature in Kelvin. The K_L is the thermodynamic equilibrium constant.

In this study, the experiments were carried out at 298, 308 and 313 K with a solution concentration of 50 mg/L of Pb(II) for GO and 100 mg/L for rGO. Linear plots of $\ln K_L$ vs $1/T$ for Pb(II) adsorption on prepared GO and rGO are shown

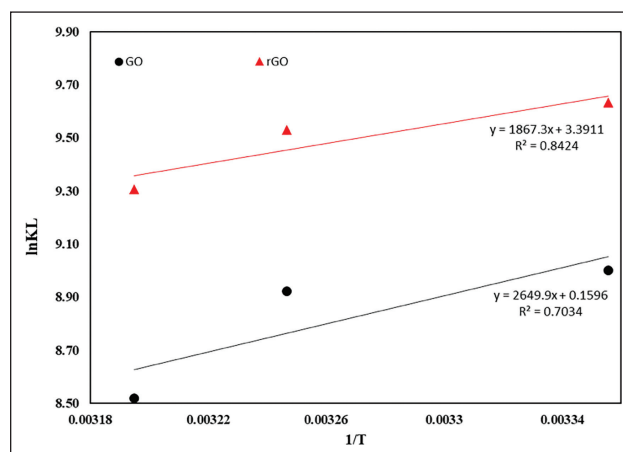


Figure 16. Thermodynamic studies for adsorption of Pb(II) by the GO and rGO materials.

in Figure 16. ΔH and ΔS were calculated from the slopes and intercepts of the plot of $\ln K_L$ vs $1/T$ by using eq 15.

The negative values of ΔG^0 for both materials show that the adsorption processes are spontaneous. The negative value of ΔH^0 infers the exothermic behavior of the adsorption. The positive value ΔS^0 indicate the increasing

Table 4. Thermodynamic Parameters for the Adsorption of Pb(II) on graphene oxide and reduced graphene oxide

Material	T (K)	ΔG (kJ mol ⁻¹)	ΔH° /kJ mol ⁻¹	ΔS° /J mol ⁻¹ K ⁻¹
rGO	298	-23.866	-15.525	28.194
	308	-24.400		
	313	-24.217		
GO	298	-22.299	-22.031	1.327
	308	-22.850		
	313	-22.165		

randomness at the solid/solution interface during the adsorption process. Related values of thermodynamic parameters were listed in Table 4.

In order to have an idea about the adsorption mechanism, the enthalpy and the size of the free energy change are used. Generally, the magnitude of ΔH° is less than 20 kJ/mol for absolute physical adsorption, while this value is in the range of 80–200 kJ/mol for chemical adsorption [55].

In general, the absolute magnitude of the change in Gibbs free energy for physisorption is between -20 and 0 kJ/mol, and chemisorption is in the range of -80 to -400 kJ/mol [56]. The results found for rGO and GO are in the range from -24.217 to -23.866 and -22.165 to -22.850 kJ/mol, respectively. These values are in the between physisorption and chemisorption [57]. It can be evaluated that physical adsorption was improved by a chemical effect. In addition, since ΔG° values are between 20 and 80 kJ/mol, adsorption type can be explained as ion exchange. Presumably the ion-exchange has a range from -20 to -80 kJ/mol [58, 59]. It can be concluded that the adsorption process is carried out with the control of several mechanisms together.

CONCLUSION

In the current study, GO was synthesized from graphite powder by Tour's method, which is a green method among the others and did not generate toxic gases during synthesis, and then non-toxic reducing agent L-ascorbic acid was used to obtain reduced graphene oxide. Both materials were characterized and compared by various methods. XRD results showed that the oxidation of graphite has given highly oxidized GO with a 10.37 Å interlayer space and decreased to 3.53 Å after the reduction of rGO by L-ascorbic acid. In addition, ATR-FT-IR analysis revealed that oxygen-containing functional groups present in GO were disappeared or decreased in intensity when converted to rGO. Wrinkled morphology was shown via SEM images and EDS analyses confirmed following reduction of GO to rGO; ratio of carbon content to oxygen content increases from 0.87 to 3.31. The intensity ratio D band to G band of rGO was higher than GO due to the removal of oxygen moieties and

restoration of sp² carbon networks during the reduction which is confirmed by Raman spectroscopy. Pb(II) removal experiments by GO and rGO were done and investigated the effect of parameters such as solution pH, contact time, initial Pb(II) concentration and temperature. Obtained results from fitting the experimental data Langmuir model showed a suitable correlation ($R^2=0.949$) and the maximum adsorbing capacity of GO was found to be 117.6 mg/g while Dubinin-Radushkevich model offered a proper correlation ($R^2=0.971$) and the maximum adsorbing capacity of rGO was calculated to be 138.5 mg/g. In addition, thermodynamic parameters showed that the adsorption of Pb(II) ions is spontaneous and exothermic in nature.

Due to their high toxicity, the removal of Pb(II) ions from aqueous solution is vital for the remedy of environmental pollution. Considering the characterization and adsorption results of green synthesized GO and rGO, it is clearly understood that they are promising and environmentally friendly alternative adsorbent materials and have high adsorption capacity for Pb(II) ions. The outcomes of present investigation hint that both GO and rGO have the potential of being effective adsorbents of removal of heavy metal ions from large volumes of aqueous solutions in the pollutant cleanup.

DATA AVAILABILITY STATEMENT

The authors confirm that the data that supports the findings of this study are available within the article. Raw data that support the finding of this study are available from the corresponding author, upon reasonable request.

CONFLICT OF INTEREST

The authors declared no potential conflicts of interest with respect to the research, authorship, and/or publication of this article.

ETHICS

There are no ethical issues with the publication of this manuscript.

REFERENCES

- [1] D. Paul, "Research on heavy metal pollution of river Ganga: A review," *Annals of Agrarian Science*, Vol. 15, 2, pp. 278–286, 2017. [\[CrossRef\]](#)
- [2] L. Hu, Z. Yang, L. Cui, Y. Lia, H. H. Ngo, Y. Wang, Q. Wei, H. Ma, L. Yan, and B. Du, "Fabrication of hyperbranched polyamine functionalized graphene for high-efficiency removal of Pb(II) and methylene blue," *Chemical Engineering Journal*, Vol. 287, pp. 545–556, 2016. [\[CrossRef\]](#)
- [3] L. Järup, "Hazards of heavy metal contamination," *British Medical Bulletin*, Vol. 68, pp. 167–182, 2003. [\[CrossRef\]](#)

- [4] F. Perreault, A. Fonseca De Faria, and M. Elimelech, “Environmental applications of graphene-based nanomaterials,” *Chemical Society Reviews*, Vol. 44(16), pp. 5861–5896, 2015. [\[CrossRef\]](#)
- [5] T. S. Vo, “Progresses and expansions of chitosan-graphene oxide hybrid networks utilizing as adsorbents and their organic dye removal performances: A short review,” *Journal of the Turkish Chemical Society Section A: Chemistry*, Vol. 8(4), pp. 1121–1136, 2021. [\[CrossRef\]](#)
- [6] Z. H. Huang, X. Zheng, W. Lv, M. Wang, Q. H. Yang, and F. Kang, “Adsorption of lead(II) ions from aqueous solution on low-temperature exfoliated graphene nanosheets,” *Langmuir*, Vol. 27, 12, pp. 7558–7562, 2011. [\[CrossRef\]](#)
- [7] S. Yu, X. Wang, X. Tan, and X. Wang, “Sorption of radionuclides from aqueous systems onto graphene oxide-based materials: A review,” *Inorganic Chemistry Frontiers*, Vol. 2(7), pp. 593–612, 2015. [\[CrossRef\]](#)
- [8] A. K. Mishra, and S. Ramaprabhu, “Functionalized graphene sheets for arsenic removal and desalination of sea water,” *Desalination*, Vol. 282, pp. 39–45, 2011. [\[CrossRef\]](#)
- [9] B. C. Brodie, “On the atomic weight of graphite,” *Philosophical Transactions of the Royal Society of London*, Vol. 149, pp. 249–259, 1859. [\[CrossRef\]](#)
- [10] W.S. Hummers Jr, R. E. Offeman, W. S. Hummers, and R. E. Offeman, “Preparation of graphitic oxide,” *Journal of the American Chemical Society*, Vol. 80(6), Article 1339, 1958. [\[CrossRef\]](#)
- [11] D. C. Marcano, D. V. Kosynkin, J. M. Berlin, A. Sinitskii, Z. Sun, A. Slesarev, L. B. Alemany, W. Lu, and J. M. Tour, “Improved synthesis of graphene oxide,” *ACS Nano*, Vol. 4(8), pp. 4806–4814, 2010. [\[CrossRef\]](#)
- [12] S. Stankovich, D. A. Dikin, R. D. Piner, K. A. Kohlhaas, A. Kleinhammes, Y. Jia, Y. Wu, S. B. T. Nguyen, and R. S. Ruoff, “Synthesis of graphene-based nanosheets via chemical reduction of exfoliated graphite oxide,” *Carbon*, Vol. 45(7), pp. 1558–1565, 2007. [\[CrossRef\]](#)
- [13] R. Hu, S. Dai, D. Shao, A. Alsaedi, B. Ahmad, and X. Wang, “Efficient removal of phenol and aniline from aqueous solutions using graphene oxide/poly-pyrrole composites,” *Journal of Molecular Liquids*, Vol. 203, pp. 80–89, 2015. [\[CrossRef\]](#)
- [14] M. J. Fernández-Merino, L. Guardia, J. I. Paredes, S. Villar-Rodil, P. Solís-Fernández, A. Martínez-Alonso, and J. M. D. Tascón, “Vitamin C is an ideal substitute for hydrazine in the reduction of graphene oxide suspensions,” *Journal of Physical Chemistry C*, Vol. 114, 14, pp. 6426–6432, 2010. [\[CrossRef\]](#)
- [15] K. K. H. De Silva, H. H. Huang, R. K. Joshi, and M. Yoshimura, “Chemical reduction of graphene oxide using green reductants,” *Carbon*, Vol. 119, pp. 190–199, 2017. [\[CrossRef\]](#)
- [16] M. Fathy, A. Gomaa, F. A. Taher, M. M. El-Fass, and A. E. H. B. Kashyout, “Optimizing the preparation parameters of GO and rGO for large-scale production,” *Journal of Materials Science*, Vol. 51(12), pp. 5664–5675, 2016. [\[CrossRef\]](#)
- [17] M. Zhao, Y. Xu, C. Zhang, H. Rong, and G. Zeng, “New trends in removing heavy metals from wastewater,” *Applied Microbiology and Biotechnology*, Vol. 100(15), pp. 6509–6518, 2016. [\[CrossRef\]](#)
- [18] S. Z. N. Ahmad, W. N. W. Salleh, N. Yusof, M. Yusop, M. Zamri, H. Rafidah, A. Nor Asikin, I. Nor Hafiza, R. Norafiqah, S. Norazlianie, and I. A. Fauzi, “Pb(II) removal and its adsorption from aqueous solution using zinc oxide/graphene oxide composite,” *Chemical Engineering Communications*, Vol. 208(5), pp. 646–660, 2021. [\[CrossRef\]](#)
- [19] T. S. Vo, M. M. Hossain, H. M. Jeong, and K. Kim, “Heavy metal removal applications using adsorptive membranes,” *Nano Convergence*, Vol. 7(1), Article 36, 2020. [\[CrossRef\]](#)
- [20] X. Wang, S. Yu, J. Jin, H. Wang, N. S. Alharbi, A. Alsaedi, T. Hayat, and X. Wang, “Application of graphene oxides and graphene oxide-based nanomaterials in radionuclide removal from aqueous solutions,” *Science Bulletin*, Vol. 61(20), pp. 1583–1593, 2016. [\[CrossRef\]](#)
- [21] S. Ahmed, S. Chughtai, and M. A. Keane, “The removal of cadmium and lead from aqueous solution by ion exchange with Na-Y zeolite,” *Separation and Purification Technology*, Vol. 13(1), pp. 57–64, 1998. [\[CrossRef\]](#)
- [22] B. E. Reed, and S. Arunachalam, “Use of granular activated carbon columns for lead removal,” *Journal of Environmental Engineering*, Vol. 120(2), pp. 416–436, 1994. [\[CrossRef\]](#)
- [23] G. Jyotsna, K. Kadirvelu, C. Rajagopal, and V. K. Garg, “Removal of lead(II) from aqueous solution by adsorption on carbon aerogel using a response surface methodological approach,” *Industrial & Engineering Chemistry Research*, Vol. 44(7), pp. 1987–1994, 2005. [\[CrossRef\]](#)
- [24] S. G. Wang, W. X. Gong, X. W. Liu, Y. W. Yao, B. Y. Gao, and Q. Y. Yue, “Removal of lead(II) from aqueous solution by adsorption onto manganese oxide-coated carbon nanotubes,” *Separation and Purification Technology*, Vol. 58(1), pp. 17–23, 2007. [\[CrossRef\]](#)
- [25] H. V. Tran, L. D. Tran, and T. N. Nguyen, “Preparation of chitosan/magnetite composite beads and their application for removal of Pb(II) and Ni(II) from aqueous solution,” *Materials Science and Engineering C*, Vol. 30(2), pp. 304–310, 2010. [\[CrossRef\]](#)

- [26] S. Doyurum and A. Çelik, "Pb(II) and Cd(II) removal from aqueous solutions by olive cake," *Journal of Hazardous Materials*, Vol. 138(1), pp. 22–28, 2006. [CrossRef]
- [27] C. Xu, X. Shi, A. Ji, L. Shi, C. Zhou, and Y. Cui, "Fabrication and characteristics of reduced graphene oxide produced with different green reductants," *PLoS ONE*, Vol. 10(12), pp. e0144842, 2015. [CrossRef]
- [28] T. S. Vo, and T. T. B. C. Vo, "Graphene oxide-covered melamine foam utilizing as a hybrid foam toward organic dye removal and recyclability," *Progress in Natural Science: Materials International*, Vol. 32(3), pp. 296–303, 2022. [CrossRef]
- [29] T. S. Vo, M. M. Hossain, T. Lim, J. W. Suk, S. Choi, and K. Kim, "Graphene oxide-chitosan network on a dialysis cellulose membrane for efficient removal of organic dyes," *ACS Applied Bio Materials*, Vol. 5(6), pp. 2795–2811, 2022. [CrossRef]
- [30] J. J. Zhang, H. Yang, G. Shen, P. Cheng, J. J. Zhang, and S. Guo, "Reduction of graphene oxide via ascorbic acid," *Chemical Communications*, Vol. 46, 7, pp. 1112–1114, 2010. [CrossRef]
- [31] B. Li, T. Liu, Y. Wang, and Z. Wang, "ZnO/graphene-oxide nanocomposite with remarkably enhanced visible-light-driven photocatalytic performance," *Journal of Colloid and Interface Science*, Vol. 377, pp. 114–121, 2012. [CrossRef]
- [32] R. K. Upadhyay, N. Soin, G. Bhattacharya, S. Saha, A. Barman, and S. S. Roy, "Grape extract assisted green synthesis of reduced graphene oxide for water treatment application," *Materials Letters*, Vol. 160, pp. 355–358, 2015. [CrossRef]
- [33] X. Geng, Y. Guo, D. Li, W. Li, C. Zhu, X. Wei, M. Chen, S. Gao, S. Qiu, Y. Gong, L. Wu, M. Long, M. Sun, G. Pan and L. Liu, "Interlayer catalytic exfoliation realizing scalable production of large-size pristine few-layer graphene," *Scientific Reports*, Vol. 3, pp. 1–6, 2013. [CrossRef]
- [34] H. Raghubanshi, S. M. Ngobeni, A. O. Osikoya, N. D. Shooto, C. W. Dikio, E. B. Naidoo, E. D. Dikio, R. K. Pandey, and R. Prakash, "Synthesis of graphene oxide and its application for the adsorption of Pb²⁺ from aqueous solution," *Journal of Industrial and Engineering Chemistry*, Vol. 47, pp. 169–178, 2017. [CrossRef]
- [35] K. K. H. De Silva, H. H. Huang, and M. Yoshimura, "Progress of reduction of graphene oxide by ascorbic acid," *Applied Surface Science*, Vol. 447, pp. 338–346, 2018. [CrossRef]
- [36] V. Sharma, Y. Jain, M. Kumari, R. Gupta, S. K. Sharma, and K. Sachdev, "Synthesis and characterization of graphene oxide (GO) and reduced graphene oxide (rGO) for gas sensing application," *Macromolecular Symposia*, Vol. 376(1), pp. 1–5, 2017. [CrossRef]
- [37] N. F. T. Arifin and M. Aziz, "Effect of reduction time on optical properties of reduced graphene oxide," *Jurnal Teknologi*, Vol. 79(1–2), pp. 25–28, 2017. [CrossRef]
- [38] S. Pei and H. M. Cheng, "The reduction of graphene oxide," *Carbon*, Vol. 50(9), pp. 3210–3228, 2012.
- [39] R. Muzyka, S. Drewniak, T. Pustelny, M. Chrubasik, and G. Gryglewicz, "Characterization of graphite oxide and reduced graphene oxide obtained from different graphite precursors and oxidized by different methods using Raman spectroscopy," *Materials*, Vol. 11(7), Article 1050, 2018. [CrossRef]
- [40] F. Gordon-Nuñez, K. Vaca-Escobar, M. Villacís-García, L. Fernández, A. Debut, M. B. Aldás-Sandoval, and P. J. Espinoza-Montero, "Applicability of goethite/reduced graphene oxide nanocomposites to remove lead from wastewater." *Nanomaterials*, Vol. 9(11), Article 1580, 2019. [CrossRef]
- [41] Y. A. Akbas, S. Yusan, S. Sert, and S. Aytas, "Sorption of Ce(III) on magnetic/olive pomace nanocomposite: isotherm, kinetic and thermodynamic studies," *Environmental Science and Pollution Research*, pp. 56782–56794, 2021. [CrossRef]
- [42] S. Z. N. Ahmad, W. N.W. Salleh, N. Yusof, M. Z. M. Yusop, R. Hamdan, N. A. Awang, N. H. Ismail, N. Rosman, N. Sazali, and A. F. Ismail, "Pb(II) removal and its adsorption from aqueous solution using zinc oxide/graphene oxide composite," *Chemical Engineering Communications*, Vol. 208, pp. 646–660, 2021. [CrossRef]
- [43] M. A. Farghali, M. M. Abo-Aly, and T. A. Salaheldin, "Modified mesoporous zeolite-A/reduced graphene oxide nanocomposite for dual removal of methylene blue and Pb²⁺ ions from wastewater," *Inorganic Chemistry Communications*, Vol. 126, Article 108487, 2021. [CrossRef]
- [44] X. Wang, W. Cai, S. Liu, G. Wang, Z. Wu, and H. Zhao, "ZnO hollow microspheres with exposed porous nanosheets surface: Structurally enhanced adsorption towards heavy metal ions," *Colloids and Surfaces A: Physicochemical and Engineering Aspects*, Vol. 422, pp. 199–205, 2013. [CrossRef]
- [45] K. Y. Kumar, H. B. Muralidhara, Y. A. Nayaka, J. Balasubramanyam, and H. Hanumanthappa, "Low-cost synthesis of metal oxide nanoparticles and their application in adsorption of commercial dye and heavy metal ion in aqueous solution," *Powder Technology*, Vol. 246, pp. 125–136, 2013. [CrossRef]
- [46] W. Konicki, M. Aleksandrak, D. Moszyński, and E. Mijowska, "Adsorption of anionic azo-dyes from aqueous solutions onto graphene oxide: Equilibrium, kinetic and thermodynamic studies," *Journal of Colloid and Interface Science*, Vol. 496, pp. 188–200, 2017. [CrossRef]

- [47] A. Dada, A. Olalekan, A. Olatunya, and O. Dada, “Langmuir, freundlich, temkin and dubinin–radushkevich isotherms studies of equilibrium sorption of Zn²⁺ onto phosphoric acid modified rice Husk,” *IOSR Journal of Applied Chemistry*, Vol. 3(1), pp. 38–45, 2012. [\[CrossRef\]](#)
- [48] S. Aytas, S. Yusan, S. Sert, and C. Gok, “Preparation and characterization of magnetic graphene oxide nanocomposite (GO-Fe₃O₄) for removal of strontium and cesium from aqueous solutions,” *Characterization and Application of Nanomaterials*, Vol. 4(1), pp. 63–76, 2021. [\[CrossRef\]](#)
- [49] Z.-H. Huang, X. Zheng, W. Lv, M. Wang, Q.-H. Yang, and F. Kang, “Adsorption of lead (II) ions from aqueous solution on low-temperature exfoliated graphene nanosheets,” *Langmuir*, Vol. 27(12), pp. 7558–7562, 2011. [\[CrossRef\]](#)
- [50] Z. Han, Z. Tang, S. Shen, B. Zhao, G. Zheng, and J. Yang, “Strengthening of graphene aerogels with tunable density and high adsorption capacity towards Pb²⁺,” *Scientific Reports*, Vol. 4, pp. 1–6, 2014. [\[CrossRef\]](#)
- [51] Z. Dong, D. Wang, X. Liu, X. Pei, and J. Jin, “Bio-inspired surface- functionalization of graphene oxide for the adsorption of organic dyes and heavy metal ions with a superhigh capacity,” *Journal of Materials Chemistry A*, Vol. 2, pp. 5034–5040, 2014. [\[CrossRef\]](#)
- [52] Y. Chen, L. Chen, H. Bai, and L. Li, “Graphene oxide-chitosan composite hydrogels as broad-spectrum adsorbents for water purification,” *Journal of Materials Chemistry*, Vol. 1, pp. 1992–2001, 2013. [\[CrossRef\]](#)
- [53] R. Karan, S. Rathour, and J. Bhattacharya, “A green approach for single-pot synthesis of graphene oxide and its composite with Mn₃O₄,” *Applied Surface Science*, Vol. 437(3), pp. 41–50, 2018. [\[CrossRef\]](#)
- [54] L. Hao, H. Song, L. Zhang, X. Wan, Y. Tang, and Y. Lv, “SiO₂/graphene composite for highly selective adsorption of Pb(II) ion,” *Journal of Colloid and Interface Science*, Vol. 369, 1, pp. 381–387, 2012. [\[CrossRef\]](#)
- [55] E. S. Aziman, A. H. J. Mohd Salehuddin, and A. F. Ismail, “Remediation of thorium (IV) from wastewater: Current status and way forward,” *Separation & Purification Reviews*, pp. 1–26, 2019. [\[CrossRef\]](#)
- [56] M. J. Jaycock and G. D. Parfitt, “Chemistry of interfaces,” Ellis Horwood Ltd., Onichester, 1981.
- [57] Y. Li, C. Wang, Z. Guo, C. Liu, and W. Wu, “Sorption of thorium(IV) from aqueous solutions by graphene oxide,” *Journal of Radioanalytical and Nuclear Chemistry*, Vol. 299(3), pp. 1683–1691, 2014. [\[CrossRef\]](#)
- [58] S. Yusan, C. Gok, S. Erenturk, and S. Aytas, “Adsorptive removal of thorium (IV) using calcined and flux calcined diatomite from Turkey: Evaluation of equilibrium, kinetic and thermodynamic data,” *Applied Clay Science*, Vol. 67–68, pp. 106–116, 2012. [\[CrossRef\]](#)
- [59] G. Gereli, Y. Seki, İ. M. Kuşoğlu, and K. Yurdakoç, “Equilibrium and kinetics for the sorption of promethazine hydrochloride onto K10 montmorillonite,” *Journal of Colloid and Interface Science*, Vol. 299, 1, pp. 155–162, 2006. [\[CrossRef\]](#)